A Broad-Band Frequency Divider Using Microwave Varactors

ROBERT G. HARRISON

Abstract—**A novel configuration using GaAs varactors in a balanced circuit configuration incorporating both coplanar waveguide and microstrip elements permits the construction of microwave frequency dividers which have near-octave divide-by-two bandwidth and excellent response to pulsed RF inputs.**

List of Symbols

c	Velocity of light *in vacuo*.
C_0	Average varactor capacitance.
$C_j(0)$	Varactor junction capacitance at zero bias.
C_p	Varactor package capacitance.
$f_c(0)$	Varactor cutoff frequency.
f_{in}	Input frequency.
$\frac{1}{2}f_{in}$	Half the input frequency.
f_0	Resonance frequency.
H	Substrate height.
j	$\sqrt{-1}$.
l	Length of transmission line.
P_{in}	Input power.
P_{out}	Output power.
Q	Quality factor.
S	Spacing between coupled lines.
v	Phase velocity.
V_b	Bias voltage.
W	Width of transmission line.
Y_{oe}	Even-mode admittance.
Y_{oo}	Odd-mode admittance.
Y'_{oo}	Y_{oo} evaluated for $\varepsilon_r = 1.0$.
Z_{oo}	Odd-mode impedance.
Z_{oe}	Even-mode impedance.
ε	Dielectric constant.
ε_r	Relative dielectric constant.
θ	Electrical length.
λ	Wavelength.
π	3.141592654.
ω	Angular frequency.
ω_0	Angular frequency of resonance.

I. Introduction

EXISTING microwave frequency dividers tend to have either good response to RF pulses but narrow bandwidth [1], or broad bandwidth but poor pulse response [2]. Previous investigations by the author [3] showed that near-octave bandwidth with good pulse response could be obtained at MHz frequencies using balanced varactor subharmonic resonators. The work described in this paper shows that this performance can be obtained at GHz frequencies also. Frequency dividers of this type are potentially important in applications where RF pulses must be translated to lower frequencies for analog or digital processing or where microwave sources must be locked to low-frequency references. Other applications include frequency counters, frequency synthesizers and FM bandwidth compressors.

Experience with varactor frequency dividers of several different designs showed that an attempt should be made to meet the objectives given below.

1) The basic resonant circuit should have a reasonably high Q and a small physical size. It should be resonant at the output frequency $\frac{1}{2}f_{in}$ and should be constructed in such a way as to minimize radiation of the input frequency f_{in} to the output port.

2) The basic resonant circuit should be balanced with respect to the output frequency $\frac{1}{2}f_{in}$ but unbalanced with respect to the input frequency f_{in}. Transformation of the balanced output signal $\frac{1}{2}f_{in}$ to the unbalanced output port should be accomplished without significantly affecting the resonator balance.

3) To avoid problems associated with mounting and bonding unpackaged chip varactors, packaged devices should be used.

These requirements can be satisfied by a balanced coupled-line microstrip resonant structure in combination with a coplanar balance-to-unbalance transformer (balun).

II. Structure

Fig. 1 shows the basic layout. A microstrip resonator consists of a pair of coupled lines capacitively loaded by matched GaAs varactors. The combination forms a bridge circuit.

The capacitive loading has the following beneficial effects:

1) The lengths of the lines are less than $\lambda/4$ at resonance. This improves the bandwidth, as pointed out by Cristal and Matthaei [4].

2) The coupling becomes predominantly magnetic. This permits the lines to be relatively far apart.

It is preferable to use a balanced circuit rather than a filter to remove the even-order harmonics of the $\frac{1}{2}f_{in}$ output. This is because, for an octave bandwidth divider, the desired $\frac{1}{2}f_{in}$ output at the top end of the band is the same frequency as the undesired f_{in} output (second harmonic of $\frac{1}{2}f_{in}$ plus feedthrough of input) at the low end of the band, i.e., the filter would be undesignable. In a sufficiently well-balanced design the absence of additional energy-storage elements

Manuscript received May 13, 1977; revised June 18, 1977. This work was supported by the Department of National Defence, DREO, Ottawa, Canada, under Contract OSR5-0030.

The author was with RCA Limited, Ste-Anne-de-Bellevue, Quebec, Canada. He is now with Com Dev Limited, 582 Orly Avenue, Dorval, Quebec, Canada H9P 1E9.

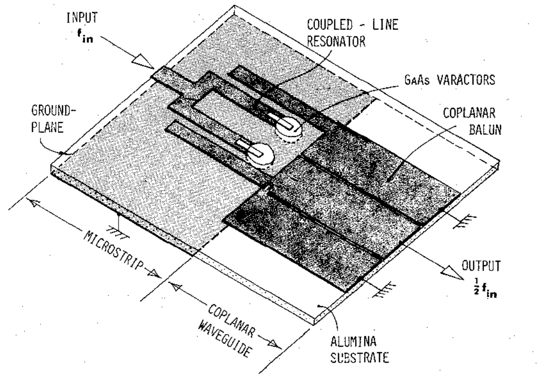

Fig. 1. Basic layout of balanced varactor frequency divider.

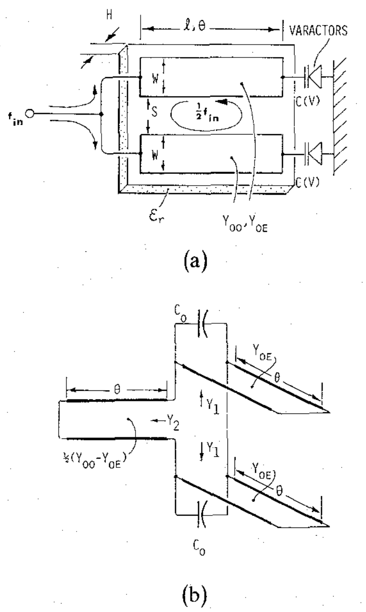

Fig. 2. (a) Microstrip/varactor coupled-line subharmonic resonator. (b) Open-wire equivalent circuit at $\frac{1}{2}f_{in}$.

would also improve the performance under conditions of pulsed RF input.

An input f_{in} divides equally between the lines so that they have potentials equal in magnitude and sign. At this frequency the lines are uncoupled and the propagation is determined by the even-mode admittance. The resonator supports oscillations at $\frac{1}{2}f_{in}$, energy being transferred from f_{in} to $\frac{1}{2}f_{in}$ via the nonlinear reactances of the varactors. At the frequency $\frac{1}{2}f_{in}$, the resonant behavior is determined by the odd-mode admittance Y_{oo} of the line-pair.

An outer pair of lines couples the balanced $\frac{1}{2}f_{in}$ signal to a coplanar-waveguide balun transformer of the type described by DeBrecht [5]. The 3-strip balun, which operates without a ground-plane, converts the balanced $\frac{1}{2}f_{in}$ signal to an unbalanced output.

III. Design of a Frequency Divider

If the influence of the output network is neglected, the basic resonant circuit of the divider is as shown in Fig. 2(a). It consists of a coupled pair of adjacent lines of equal electrical length θ. Each line is reactively loaded with a varactor the average capacitance of which is C_0 at the bias voltage V_b. Y_{oo} and Y_{oe} are the odd-mode and even-mode admittances for each line. Since the common input point to the coupled lines is a voltage null at $\frac{1}{2}f_{in}$, the open-wire equivalent circuit of Fig. 2(b) can be found by the method of Sato and Cristal [6]. The indicated admittances are

$$Y_1 = j\omega C_0 - jY_{oe} \cot \theta \tag{1}$$

$$Y_2 = -j\tfrac{1}{2}(Y_{oo} - Y_{oe}) \cot \theta \tag{2}$$

and the condition for *small-signal* resonance at output frequency $f_o = \omega_0/2\pi$ is

$$Y_1 + 2Y_2 = 0. \tag{3}$$

This gives

$$\omega_0 C_0 = Y_{oo} \cot \theta \tag{4}$$

as the odd-mode resonance condition. Note that the even-mode admittance Y_{oe} does not appear in this expression.

The required electrical length l of the lines may be found as follows:

1) select values of line-width W and line-spacing S for a given substrate thickness H;
2) using the data given by Weiss and Bryant [7] find the odd-mode coupled line admittances Y_{oo} and Y'_{oo} using the dielectric constant $\varepsilon = \varepsilon_r$ for the substrate material and $\varepsilon = 1.0$ for vacuum, respectively;
3) since $\theta = \omega_0 l/v$ and the phase velocity is $v = cY'_{oo}/Y_{oo}$, equation (4) gives

$$l = \frac{c}{\omega_0} \frac{Y'_{oo}}{Y_{oo}} \arctan\left(\frac{Y_{oo}}{\omega_0 C_0}\right) \tag{5}$$

as the required electrical length.

Experimental and theoretical investigations show that the behavior of nonlinear resonators of the type considered here is different from that of linear resonators in several important respects.

a) The resonant behavior is a function of the signal level. In general the resonance bandwidth increases rapidly as the signal level increases.

b) The resonance is not symmetrical with respect to frequency; the major part of the bandwidth increase with signal level occurs at frequencies *below* the small-signal resonance ω_0. Theory shows that this is true even if the resonator has an arbitrarily high Q, i.e., the broad bandwidth does not depend on the presence of damping.

These considerations mean that the resonator should be designed so that the required maximum output frequency occurs at or near the small-signal resonance frequency f_0.

IV. Practical Example

The objective was to design a frequency divider to accommodate an input bandwidth of approximately 4.0–8.0 GHz. Accordingly, the small-signal resonance frequency f_o was made ~4 GHz.

For maximum bandwidth, the resonator size should be minimized. Because of the capacitive loading l can be $\leq \lambda/8$.

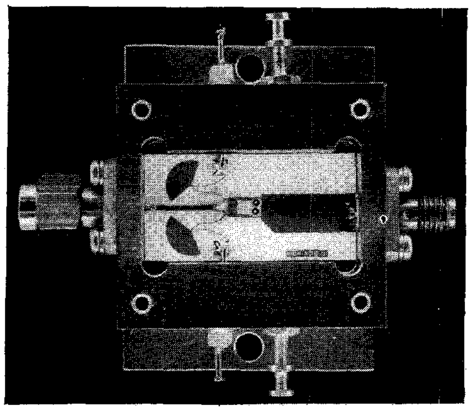

Fig. 3. Actual view of broad-band frequency divider for 4- to 8-GHz input frequency range. Substrate dimensions are 28 × 14 mm.

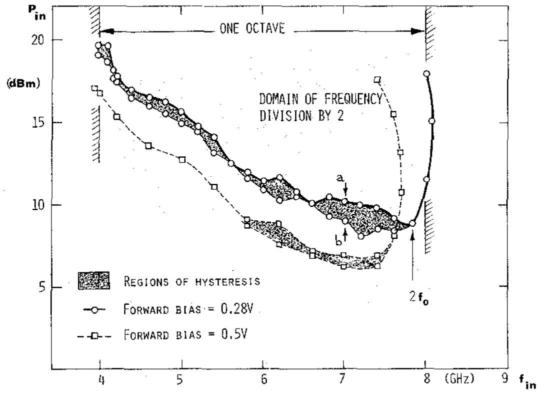

Fig. 4. Domain of frequency division, shown for two different values of bias V_b.

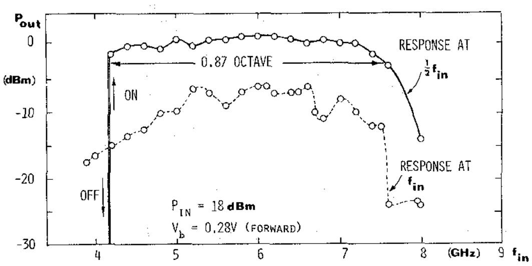

Fig. 5. Frequency responses at $\frac{1}{2}f_{in}$ and at f_{in} for a fixed input level.

W was made 0.13 mm; minimum S was fixed by the varactor[1] diameter at 0.83 mm. Using an alumina substrate with $H = 0.635$ mm, $\varepsilon_r \sim 9$, one finds $Y_{oo} = 0.011$ mho and $Y'_{oo} = 0.0047$ mho. For varactors with $C_j(0) = 0.375$ pF, $C_p = 0.138$ pF, equation (5) gives $l = 3.56$ mm. The outer lines were 0.13 mm wide and were spaced 0.13 mm from the inner lines. Varactor cutoff frequency was $f_c(0) \sim 260$ GHz.

Fig. 3 shows the complete divider. A dc blocking capacitor isolates the 50-ohm input line from the resonator. The four curved high-impedance lines are each $\lambda/4$ at the 6-GHz input center frequency. The fan-shaped radial lines produce broadband shorts at the junction of each pair of high-impedance lines. Two bias circuits permit independent varactor biasing to optimize balance (separate chip capacitors would be used). Substrate dimensions are 28 × 14 mm. The carrier includes a cavity beneath the coplanar balun. According to [5] the balun has odd and even mode impedances $Z_{oo} = 55$ ohms, $Z_{oe} = 49$ ohms. The balun length is $\lambda/4$ at the 3-GHz output center frequency.

V. Measured Results

A. Region of Frequency Division

Fig. 4 shows the region of frequency division. A minimum level of input power P_{in} is required for output at $\frac{1}{2}f_{in}$. Consider the region for $V_b = 0.28$ V forward bias, which gives maximum bandwidth. Let f_{in} be 7 GHz. Then as P_{in} increases from zero, frequency division commences abruptly at point "a." If P_{in} is reduced, the $\frac{1}{2}f_{in}$ output persists down to point "b," where it suddenly drops to zero. This hysteresis region is shown as the shaded area.

Fig. 4 also shows the effect of increasing V_b to 0.5 V. A reduction in threshold levels is accompanied by a reduction in the maximum operating frequency due to an increase in the average varactor capacitance.

B. Frequency Response

Fig. 5 depicts the frequency response for a fixed P_{in}. As would be expected from Fig. 4, the bandwidth increases as P_{in} increases. A high P_{in} is chosen here to obtain near-octave division bandwidth. For narrower bandwidths, P_{in} can be reduced. Further reductions in P_{in} can be obtained by increasing the forward V_b. (In another design, narrow-band operation was obtained at an input level of +2 dBm for $f_{in} = 10$ GHz). At the lower band-edge amplitude hysteresis occurs, corresponding to the shaded region of Fig. 4. Fig. 5 also shows the f_{in}-level at the output. This signal is due both to feedthrough of the input and to the resonator unbalance. Feedthrough at the high end of the band was suppressed using ferrite material in the cavity beneath the balun.

Fig. 6 shows the frequency response of the divider with a 21-dB-gain GaAs FET preamplifier. Here P_{in} is fixed at −6 dBm; the maximum P_{out} is +1 dBm. Because of the preamplifier frequency response, turnon occurs at 4.75 GHz rather than the 4.18 GHz for the divider alone.

C. Output Spectrum

The output spectrum produced in response to a fixed 6.0-GHz input frequency is given in Fig. 7. The out-of-band spurious response at 1.75 GHz is 40 dB below the $\frac{1}{2}f_{in}$ signal at 3.0 GHz. There is a similar spurious response at 4.25 GHz also. Inband spurious frequencies are 65 dB below the $\frac{1}{2}f_{in}$ signal. The behavior of the spurious responses as f_{in} is swept from 4.0 to 8.0 GHz is shown in Fig. 8. This display was obtained by driving the X-axis of an oscilloscope with a voltage proportional to f_{in}, the Y-axis with a voltage proportional to the spectrum analyzer horizontal sweep (i.e., to a selected range of f_{out} frequencies), and Z-modulating the intensity with the spectrum analyzer video output voltage.

[1] Microwave Associates type MA-48505-E-155 diffused junction epitaxial GaAs varactors.

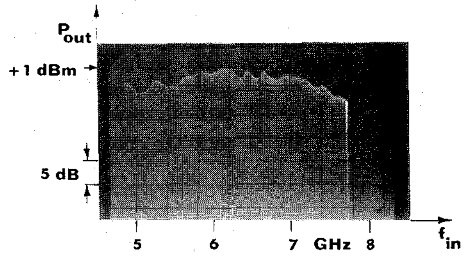

Fig. 6. Frequency response of divider with a 21-dB-gain GaAs FET preamplifier. P_{in} is -6 dBm. The $\frac{1}{2}f_{in}$ spectral line is shown as f_{in} sweeps from 4.0 to 7.7 GHz.

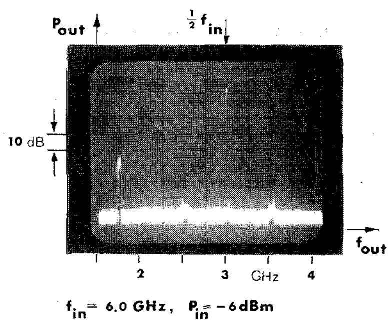

Fig. 7. Typical output spectrum showing -65-dB spurious levels in the 2.0- to 4.0-GHz output band.

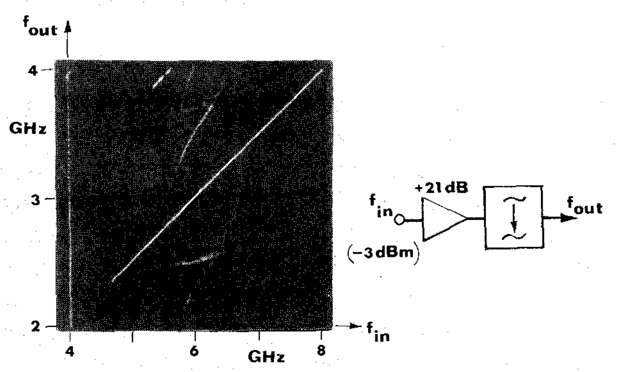

Fig. 8. Display of output spectrum versus input frequency showing divider linearity and behavior of inband spurious responses.

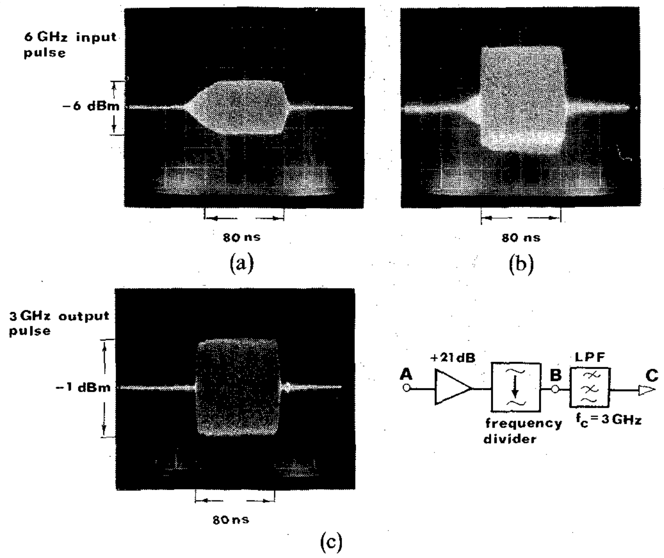

Fig. 9. (a) 6-GHz RF pulse applied to preamplifier. (b) 3-GHz RF pulse output from frequency divider. Distortion is due to residual 6-GHz feedthrough. (c) 3-GHz RF pulse output after low-pass filter, 3-GHz cutoff frequency.

Thus the display of Fig. 8 is built up of many vertical scans, each scan representing the spectrum for a particular value of f_{in}. The linearity of the f_{in}-f_{out} relationship is apparent. The behavior of the inband spurious frequencies as f_{in} is varied can also be seen. They remain at least 50 dB below the main $\frac{1}{2}f_{in}$ signal across the band.

D. RF Pulse Response

A typical response to a pulsed RF input signal is shown in Fig. 9. The RF frequency of 6 GHz lies near the center of the input band of the divider, and the pulse amplitude is sufficient for broadband operation. The measurements were made using a sampling oscilloscope with a risetime (< 30 ps) providing good response at the maximum frequency of interest, 8 GHz.

Waveform A shows the 6.0-GHz input pulse produced using a p-i-n-diode modulator, with a turn-on time of ~ 30 ns and decay time of ~ 10 ns. Since the RF signal is incoherent with respect to the pulse envelope, the individual cycles cannot be resolved. Waveform B is the output from the frequency divider. The distortion is due to the presence of residual f_{in} at the output port. After passing the output pulse through a low-pass filter the 3.0-GHz pulse waveform C is obtained. This has a turn-on time of ~ 3 ns and a turn-off time of ~ 5 ns. The turn-on delay of pulse C with respect to pulse A is apparent only. Because of the nonlinear relationship between P_{out} and P_{in}, there is no generation of $\frac{1}{2}f_{in}$ until P_{in} reaches the necessary threshold level. After that the turn on is very rapid, corresponding here to about 9 RF cycles.

VI. Conclusions

A broad-band microwave frequency divider using parametric subharmonic resonance has been demonstrated. A ± 2-dB bandwidth of 0.87 octave has been obtained without optimizing the circuit. Nonharmonically related spurious outputs are typically at least 40 dB below the main frequency-divided output signal. It should be possible to reduce the level of the input frequency at the output port both by reducing direct radiation from the input and by improving the circuit balance. The response to pulsed RF inputs is excellent, rise and fall times being typically of the order of 10 RF cycles.

Acknowledgment

The author wishes to thank Dr. T. W. Tucker of DREO for his encouragement and Dr. P. Bura, D. Cowan, and P. Mercer for many helpful discussions.

References

[1] L. C. Upadhyayula and S. Y. Narayan, "Microwave frequency dividers," *RCA Review*, vol. 34, pp. 595–607, Dec. 1973.

[2] S. V. Ahamed, J. C. Irvin, and H. Seidel, "Study and fabrication of a frequency divider-multiplier scheme for high-efficiency microwave power," *IEEE Trans. Commun. Tech.*, vol. COM-24, pp. 243–249, Feb. 1976.

[3] R. G. Harrison, "Steady state and transient phenomena in parametric subharmonic oscillators," Ph.D. dissertation, Univ. of London, July 1964.

[4] E. G. Cristal and G. L. Matthaei, "A technique for the design of multiplexers having contiguous channels," *IEEE Trans. Microwave Theory Tech.*, vol. MTT-12, pp. 88–93 (see p. 89), Jan. 1964.
[5] R. E. DeBrecht, "Coplanar balun circuits for GaAs FET high-power push-pull amplifiers," in *IEEE-GMTT Int. Microwave Symposium Digest* (Univ. of Colorado, June 1973), pp. 309–311.
[6] R. Sato and E. G. Cristal, "Simplified analysis of coupled transmission line networks," *IEEE Trans. Microwave Theory Tech.*, vol. MTT-18, pp. 122–131, Mar. 1970.
[7] J. A. Weiss and T. G. Bryant, "Even and odd mode characteristic impedance for coupled microstrip," *Microwave Engineer's Handbook*, vol. 1. Dedham, Massachusetts: Artech House, 1971, pp. 132–133.

A Nonlinear Analysis of Schottky-Barrier Diode Upconverters

MASAMI AKAIKE, MEMBER, IEEE, AND KAZUHITO OHNISHI

Abstract—**A nonlinear computer analysis of Schottky-barrier diode upconverters by means of obtaining the steady-state solutions of differential equations characterized by the diode and connected circuits is shown. Both the nonlinearities of barrier resistance and capacitance are taken into consideration. The waveforms of the voltage and current at the diode, impedance, and input–output power relationships are computed for 120-GHz upconverters.**

I. Introduction

FREQUENCY upconverters have been widely used in transmitters of the microwave and millimeter-wave transmission systems. There are two kinds of diodes used: Schottky-barrier diodes and p-n-junction varactor diodes. In varactor diode upconverters, since a sufficient dc bias voltage is applied reversely to the diode and no conduction current flows during operation, frequency conversion is performed through only the nonlinearity of the junction capacitance. In Schottky-barrier diode upconverters, however, the forward conduction current flows across the barrier during a certain period of time whereas the diode is reversely biased, and both the nonlinearities of barrier resistance and junction capacitance contribute to frequency conversion.

For designing the upconverter circuit and diode to be used, it is necessary to know their characteristics, such as the impedances, input–output power relationship, and voltage and current waveforms at the diode. For varactor upconverters, there have been excellent theoretical papers already reported,[1] and various fundamental characteristics have been made clear. As for Schottky-barrier diode upconverters, however, since the frequency conversion mechanism is related to two nonlinearities, and the current- or voltage-excitation model commonly assumed in varactor upconverters is not realistic, the treatment is more complex, and perhaps the analytical calculation is impossible.

According to the past experience on millimeter-wave upconverters, Schottky-barrier diodes exhibited better characteristics with respect to ease in circuit adjustment and suppression of unwanted spurious oscillations [1]. In the guided millimeter-wave transmission system in Japan, W-40G system, Schottky-barrier diode upconverters were preferred for that reason [2]. Although Schottky-barrier diode upconverters are believed to be very important components in practical communication systems in the microwave region and above, there have been no theoretical papers dealing with their characteristics in detail.

It is the purpose of this paper to present a theoretical investigation of Schottky-barrier diode upconverters by means of computer-aided numerical analysis. There are two approaches of analysis possible: 1) the time-domain approach in which differential equations of voltage and current, with respect to time are built, and their steady-state solutions are obtained, and 2) the frequency-domain approach in which the voltage and current components of specific frequencies are first assumed, simultaneous equations with respect to these components are made utilizing the voltage–current relationship of the diode, and then they are solved.

The time-domain approach is used in the present paper. Although this method of analysis can be used for any frequency, the present computation is performed at 120 GHz. In the analysis the following points are assumed.

1) An unencapsulated diode is directly mounted in the waveguide, i.e., the diode case capacitance is not considered. Furthermore, the equivalent circuit of the diode is somewhat simplified. The parameters of the diode used in the computation are determined by small-signal measurement. A detailed discussion is given in Section II.

Manuscript received May 17, 1977; revised July 16, 1977.
The authors are with the Yokosuka Electrical Communication Laboratory, Nippon Telegraph and Telephone Public Corporation, Yokosuka-shi, Kanagawa-ken, 238-03 Japan.

[1] There have already been published good textbooks on varactor diodes and their applications, such as H. A. Watson, *Microwave Semiconductor Devices and Their Circuit Applications*, New York: McGraw-Hill, 1969, and M. Miyagawa, *Varactor Diodes and Their Applications*, Tokyo, Japan: Industrial Daily News, Ltd., 1969. Original papers are found in these textbooks.